Double Coherence Resonance in Neuron Models Driven by Discrete Correlated Noise

Thomas Kreuz,[1,*] Stefano Luccioli,[1,2] and Alessandro Torcini[1,2]
[1]*Istituto dei Sistemi Complessi-CNR, Sesto Fiorentino, Italy*
[2]*Istituto Nazionale di Fisica Nucleare, Unitá di Firenze, Sesto Fiorentino, Italy*
(Received 12 June 2006; published 6 December 2006)

We study the influence of correlations among discrete stochastic excitatory or inhibitory inputs on the response of the FitzHugh-Nagumo neuron model. For any level of correlation, the emitted signal exhibits at some finite noise intensity a maximal degree of regularity, i.e., a coherence resonance. Furthermore, for either inhibitory or excitatory correlated stimuli, a *double coherence resonance* is observable. Double coherence resonance refers to a (absolute) maximum coherence in the output occurring for an optimal combination of noise variance and correlation. All of these effects can be explained by taking advantage of the discrete nature of the correlated inputs.

DOI: 10.1103/PhysRevLett.97.238101 PACS numbers: 87.19.La, 02.50.Fz, 05.40.−a, 87.10.+e

Excitable systems driven by fluctuations exhibit a large variety of phenomena where noise plays a constructive role. Among the most studied are stochastic resonance, the enhanced detectability of weak periodic stimuli for an intermediate noise level [1], and coherence resonance (CR), the regularization of the system response at an optimal noise intensity without any external drive [2,3]. CR has been observed in many theoretical and experimental setups such as electronic devices, semiconductor lasers, and climate models (for a recent review, cf. [4]). In neuroscience, evidence of CR has been reported for the cat's spinocortical activity [5] as well as for a variety of single neuronal models. A prominent example is the two-dimensional FitzHugh-Nagumo (FHN) model [6] that incorporates essential neuronal properties such as threshold dynamics (activation) and refractoriness.

A second type of CR with respect to the level of correlation has been observed in research areas as diverse as laser dynamics [7], digital circuits [8], chemical reactions [9], and neuronal models [10]. In computational neuroscience, continuous noise is replaced by a series of discrete random kicks representing the postsynaptic potentials (PSPs) released by excitatory and inhibitory synapses [11–15]. Correlations are then introduced via the method of shared input (cf. [11–13]) such that the correlation equals the probability that different synapses deliver PSPs at the same time. Whereas the classical CR with respect to the noise intensity can be explained by the different dependencies of slow activation and fast excitation on the noise variance [3,16,17], so far the origin of the second type of CR has remained unclear.

In this Letter, we address this issue by investigating a FHN model driven by a large number of stochastic synaptic inputs with correlations only among trains of either excitatory or inhibitory PSPs. In both cases, the system exhibits the classical CR at any level of correlation, whereas for almost all noise strengths the second type of CR can be observed. The discrete nature of the inputs allows one to vary independently correlation strength and noise intensity and, thus, to disclose the different mechanisms responsible not only for the CRs but also for the double coherence resonance (i.e., the existence of an optimal combination of noise and correlation strength for which the system responds with maximal coherence) discovered for both excitatory and inhibitory correlation.

The FHN model can be written as

$$\dot{V} = \phi\left(V - \frac{V^3}{3} - W\right), \qquad \dot{W} = V + a - I(t), \tag{1}$$

with a voltage variable V, a recovery variable W, and $I(t)$ the external synaptic input. We set time scale separation $\phi = 100$ and bifurcation parameter $a = a_0 \equiv 1.05$ so that the dynamics has only one attractor (a stable focus) but is close to the supercritical Hopf bifurcation at $a = 1$.

In this study, we consider a balanced FHN neuron in the *high-input regime* [11] with the input modeled as the superposition of an equal number $N \sim 100$–$10\,000$ of Poissonian trains of excitatory and inhibitory PSPs (EPSPs and IPSPs, respectively) with the same rate ν_0

$$I(t) = \Delta W_0\left[\sum_{i=1}^{N}\sum_{j}\delta(t - t_i^j) - \sum_{k=1}^{N}\sum_{l}\delta(t - t_k^l)\right], \tag{2}$$

where t_i^j (t_k^l) are the times of the instantaneous excitatory (inhibitory) kicks of amplitude ΔW_0. The neuron fires upon a single excitatory kick with amplitude higher than $(\Delta W)_c \simeq 0.0138$ (for $a = a_0$). However, here we consider kicks of much smaller amplitude $\Delta W_0 = 0.0014$ with rates $\nu_0 = 0.3$, 0.6, and 1.2 comparable with the firing rate $\nu_f = \nu_f(a)$ just beyond the bifurcation [18].

We examine the influence of input correlation ρ_x on the neuronal response, restricting ourselves to correlation among either excitatory ($x = e$) or inhibitory ($x = i$) inputs only. Correlations are expressed in terms of the Pearson correlation coefficient ρ_x equal to the average fraction of shared kicks delivered by each pair of synapses or, analogously, to the average fraction of synapses deliv-

ering kicks at the same time [12]. Since in our model the inputs of different synapses are not distinguishable, their effect can be reproduced by two overall kick trains corresponding to correlated and uncorrelated PSPs, respectively. While the superposition of the uncorrelated kick trains can be modeled as a single Poissonian sequence of PSPs of constant amplitude ΔW_0 and rates $\nu_u = N\nu_0 \sim 5$–1200 quite high with respect to the natural firing frequency, correlated PSPs are generated using a refined method of shared inputs (cf. [11–13]). The superposition of the correlated kick trains (with correlation ρ_x) can be represented as a unique overall Poissonian train of kicks of variable amplitude $\Delta W = n \times \Delta W_0$ and with constant rate $\nu_x = \nu_0/\rho_x$. The kick amplitude n (in units of ΔW_0) follows a binomial distribution

$$p_n^{(N)} = \frac{N!}{n!(N-n)!}\rho_x^n(1-\rho_x)^{N-n}, \tag{3}$$

with average $\langle n\rangle = \rho_x N$ and variance $\mathrm{var}[n] = \rho_x(1-\rho_x)N$. For the balanced case, the average input current is zero and does not depend on the correlation, while the current variance per unit time σ^2 is determined by the variability of both correlated and uncorrelated kick trains: $\sigma^2 = \Delta W_0^2[\langle n\rangle^2 + \mathrm{var}[n] + \langle n\rangle]/T_x$, with $T_x = \nu_x^{-1}$.

For large N, the correlated kicks can be seen as large amplitude events that are delivered at a much lower rate $\nu_x \ll \nu_u$ than the uncorrelated inputs that can be assimilated to an almost continuous background. The effect of this background consists in renormalizing the bifurcation parameter according to $\bar{a} = a_0 \pm \langle\Delta W\rangle/T_x$, the shift being positive (negative) for $x = e$ ($x = i$). The influence of the correlated kicks is embodied in the variance that for large N (at the leading order) reads as $\sigma^2 \simeq \langle\Delta W\rangle^2/T_x$. Thus, in the high-input regime the statistical properties of the response are determined once the average amplitude of the kick $\langle\Delta W\rangle$ and T_x are known.

In the following, we characterize the coherence of the neuronal response in dependence on noise strength σ^2 and correlation ρ_x (or, equivalently, T_x) [19], changing the latter from full inhibitory correlation $\rho_i = 1$ to full excitatory correlation $\rho_e = 1$ including the completely uncorrelated case $\rho_e = \rho_i = 0$. As an indication of CR, we employ the occurrence of a minimum in the coefficient of variation R at intermediate noise levels. This quantity denotes the standard deviation of the distribution of the interspike time intervals (ISIs) normalized by its mean $\bar{T}_{\mathrm{ISI}}$ and attains the value 0 for a perfectly regular signal and the value 1 for a Poissonian process.

For fixed ρ_x, the coefficient of variation R exhibits a minimum for intermediate values of σ^2 in the whole range of excitatory and inhibitory correlations (cf. Fig. 1). Depending on the type of correlation, we denote this effect as excitatory or inhibitory coherence resonance (ECR or ICR, respectively) [20]. Furthermore, by ordering the correlations from full inhibitory to full excitatory for almost all noise strengths σ^2, a minimum of R can be observed at intermediate ρ_x. Finally, in each half-plane (σ^2, ρ_x) (with $x = e$ and $x = i$, respectively), an overall minimum for R can be identified corresponding to excitatory and inhibitory double coherence resonance (EDCR and IDCR, respectively). The IDCR is also the absolute minimum.

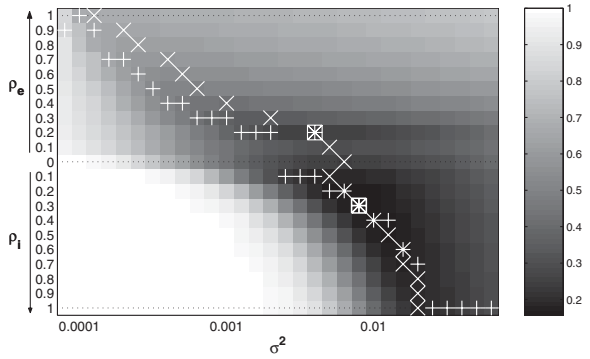

FIG. 1. Coefficient of variation R as a function of noise strength σ^2 for both excitatory (ρ_e) and inhibitory (ρ_i) correlation. For the sake of brevity, we project the axis of the two-dimensional plane (ρ_e, ρ_i) on one single axis. In each column, a white + marks the minimum for fixed variance, while a white × in each row refers to the minimum for fixed correlation (i.e., the CRs). Horizontal lines mark the cases with no correlation, $\rho_e = 1$, and $\rho_i = 1$ exhibiting CR, ECR, and ICR, respectively. Finally, the thin and thick white squares indicate the absolute minima obtained for excitatory and inhibitory correlation, i.e., the EDCR and IDCR, respectively. Data refer to $\nu_0 = 0.3$.

These effects can be better appreciated by considering the minimal value R_m for each correlation as a function of T_x (cf. Fig. 2). The curves for three different ν_0 almost

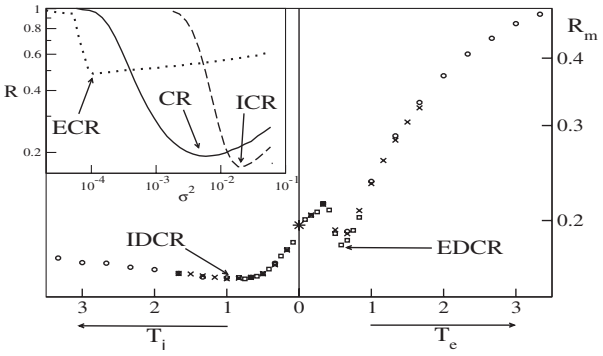

FIG. 2. Minimal values of the coefficient of variation R_m, obtained for fixed correlation, versus the period T_ρ. Data are ordered from full inhibitory correlation to full excitatory correlation. Symbols refer to different ν_0 values: 0.3 (circles), 0.6 (crosses), and 1.2 (squares). The asterisk denotes the uncorrelated case, and the arrows mark the positions of the double coherence resonances. Inset: R versus σ^2 for different correlations ($\nu_0 = 0.3$): no correlation (solid line), $\rho_e = 1$ (dotted line), and $\rho_i = 1$ (dashed line). Arrows mark the position of the respective coherence resonances.

coincide, indicating that once T_x is fixed the minima R_m occur at similar variances σ_m^2. Absolute minima are observed at finite ρ_x and σ^2 for both excitatory (EDCR at $\bar{T}_e \equiv \bar{\rho}_e/\nu_0 \simeq 0.65$) and inhibitory correlations (IDCR at $\bar{T}_i \equiv \bar{\rho}_i/\nu_0 \simeq 0.9$). This behavior of R_m is accompanied by a monotonous increase of the corresponding variances σ_m^2 when going from $\rho_e = 1$ to $\rho_i = 1$ (cf. Fig. 1). As we show in the following, not only do R_m and σ_m^2 depend on both the type and strength of correlation, but also the underlying mechanisms are completely different from one another and, in particular, from the one responsible for CR without correlation [3].

Excitatory coherence resonance.—We begin with the origin of the ECR at full excitatory correlation $\rho_e = 1$. For this case, the ISI distribution of the output can be described, for any σ^2, in terms of a Poissonian process with average period $\bar{T}_{\mathrm{ISI}}$ and refractory time T_{ref}. The expression of R is simply given by $R_P = 1 - T_{\mathrm{ref}}/\bar{T}_{\mathrm{ISI}}$; however, the course of R reveals a z-like shape with a clear minimum (the ECR cf. inset in Fig. 2). At low variances, firing resembles a noise activated process, and, therefore, $\bar{T}_{\mathrm{ISI}} \gg T_{\mathrm{ref}}$ and $R = R_P \simeq 1$. For increasing σ^2, the average kick amplitude $\langle \Delta W \rangle$ gets larger until one single EPSP may be enough to trigger a spike, thus leading to more frequent firings and to an abrupt decrease of R. This quantity reaches its minimum when a 1:1 synchronization between the EPSPs and the output spikes sets in, since now each kick is sufficient to lead the system above the firing threshold from any state of the system (except during the refractory period). Accordingly, for $\sigma^2 \geq \sigma_m^2$ the ISI distribution exhibits a tail with slope ν_e and $R = R_{\mathrm{sync}} \equiv 1 - T_{\mathrm{ref}}/T_e$. Further increasing $\langle \Delta W \rangle$ forces the system to fire even during the refractory period, thus leading to a reduction of T_{ref}, which explains the final growth of R for $\sigma^2 > \sigma_m^2$.

Excitatory double coherence resonance.—This mechanism for ECR remains valid also for decreasing correlation ρ_e until R_m reaches its local minimum at $\bar{\rho}_e$ (corresponding to the EDCR cf. Fig. 2). Beyond the EDCR, i.e., for $\rho_e < \bar{\rho}_e$, the 1:1 synchronization regime is no longer reached [cf. Fig. 3(a)]. For $\rho_e < \bar{\rho}_e$, the average kick amplitude $\langle \Delta W \rangle$ is always smaller than the minimal amplitude $(\Delta W)_c$ needed to elicit a spike [starting from the fixed point for the deterministic FHN, i.e., for Eq. (1) with $I(t) \equiv 0$]. For $\rho_e \geq \bar{\rho}_e$ and sufficiently high σ^2 (or, analogously, $\bar{a}$), the average kick always overcomes the threshold $(\Delta W)_c$, thus confirming that the regime of 1:1 synchronization is always reached. Since the minimum of R is associated with the onset of 1:1 synchronization (implying $R_m = R_{\mathrm{sync}}$), R_m decreases for $1 > \rho_e > \bar{\rho}_e$. For all correlations $[\bar{\rho}_e; 1]$, this occurs roughly for the same amplitude $\langle \Delta W \rangle \simeq \Delta W_c$ [cf. Fig. 3(a)]; thus, T_{ref} is not significantly altered and the decrease of R_m is due to the reduction of T_e with decreasing correlation. Finally, beyond the EDCR, i.e., for $\rho_e < \bar{\rho}_e$, the system is no longer strictly forced by the driving kick train with very high

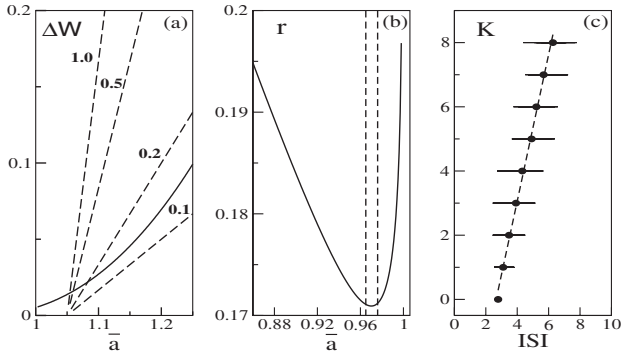

FIG. 3. Excitatory correlation: (a) Minimal amplitude $(\Delta W)_c$ (solid line) and average kick amplitude $\langle \Delta W \rangle$ (dashed lines) versus the renormalized bifurcation parameter $\bar{a}$. The numbers in proximity of the dashed lines indicate the corresponding values of ρ_e. Data refer to $\nu_0 = 0.3$, in this case $\bar{\rho}_e \sim 0.2$. Inhibitory correlation: (b) Ratio $r(\bar{a})$ for the deterministic FHN model; the values of R_m for $\rho_i > \bar{\rho}_i$ are associated with $\bar{a}$ values located within the two dashed lines for all of the examined ν_0. (c) Number of inhibitory kicks K received within a certain ISI as a function of its duration. Solid circles mark the average for each K. The dashed line indicates a linear fit; the inverse of its slope gives the delay per kick δ. Data have been obtained from 6000 ISIs for $\nu_0 = 0.3$, $\rho_i = 0.6$, and $\sigma^2 = 0.06$.

frequency, the period of firing decreases (i.e., $\bar{T}_{\mathrm{ISI}} > T_e$), and thus R_m increases.

Inhibitory coherence resonance.—Turning our attention to correlated inhibitory inputs, we start with examining the origin of the ICR at full inhibitory correlation $\rho_i = 1$. Once more at low variances, the emission of spikes is due to an activation process with $R \sim 1$. For increasing σ^2, the renormalization of the bifurcation parameter, now due to the uncorrelated EPSPs, drives the system towards the repetitive firing regime eventually crossing the bifurcation at $\bar{a} = 1$, and this leads to a fast decrease of R. On the other hand, the correlated IPSPs inhibit tonic firing, but despite the increase of their amplitude with σ^2 their action gets less effective. This is because the fraction of time $r(\bar{a})$ during which the neuron is sensitive to the arrival of a kick before a spike emission [21] decreases for increasing σ^2 (i.e., for smaller $\bar{a}$). Moreover, $r(\bar{a})$ exhibits a minimum at $\bar{a} \sim 0.97$. Noticeably, R_m is associated with corresponding $\bar{a}$ values for all $\rho_i > \bar{\rho}_i$ [cf. Fig. 3(b)]. Thus, the minimum is due to the uncorrelated kick trains that renormalize the bifurcation parameter. The final increase of R at large $\sigma^2 > \sigma_m^2$ is reflected by a ''quantization'' in the ISI distribution. The single ISI is proportional to the number of inhibitory kicks received within its duration [cf. Fig. 3(c)], and for high variances the delay per kick δ, i.e., the average retardation (with respect to the natural firing period) of the next neuronal firing induced by a single inhibitory kick, increases, and, consequently, the ISI distribution broadens, finally revealing a multimodal structure.

Inhibitory double coherence resonance.—This mechanism for ICR is still valid for decreasing correlations ρ_i

until R_m reaches its absolute minimum at $\bar{\rho}_i$ (corresponding to the IDCR cf. Fig. 2). The decrease of R_m with ρ_i is due to the fact that R_m is associated with an almost constant $\bar{a}$ value within the interval $[\bar{\rho}_i; 1]$ and that for fixed $\bar{a}$ the amplitude of the inhibitory kick $\langle \Delta W \rangle \propto \rho_i$. Consequently, the average delay per kick δ decreases with the correlation until the quantization in the ISI distribution disappears at the IDCR at $\rho_i = \bar{\rho}_i$. For smaller $\rho_i \ll \bar{\rho}_i$, the frequency of the inhibitory kicks becomes more important than their amplitudes. In particular, lowering the correlation towards the uncorrelated case leads to an increasing rate ν_i of inhibitory disturbances that renders the neuronal spiking more irregular, which in turn is reflected by the increase of R_m. In summary, we described novel mechanisms for CR that are not, as in the uncorrelated case [3], related to the different nature of the stochastic processes underlying neuronal firing at low and high noise but that rely on the discrete nature of the correlated inputs. Furthermore, we reported the existence of DCRs for both excitatory and inhibitory correlations. These DCRs reflect the change from the classical CR [3] to amplitude-dominated mechanisms responsible for the CR. While the EDCR is related to a complete synchronization with the input, the IDCR is due to a quantization of the neuronal output.

Our results indicate that the coherence in the response of an excitable system driven by fluctuations can be modulated by controlling independently the level of correlation and the noise variance. This could be of high relevance for neuronal coding, since there are indications that correlated activities (as indeed measured, e.g., among cortical neurons [22]) can influence the coding ability of neuronal populations. More recently, neuronal input correlation has been linked to changes in attention, suggesting its major impact on the information flow in the brain [23]. Remarkably, in simulations with correlated inhibitory input, it has been shown that attention (modeled as an increase of synchrony in interneuron networks) can lead to a decrease of the coefficient of variation of single output spike trains [24]. Furthermore, we have verified that the FHN model with conductance-based inputs exhibits the same coherence effects as reported here for the current-driven model. This analysis together with further extensions to more physiological setups will be the subject of future studies. Finally, since most of the reported results are not specifically related to the considered model, we expect that analogous effects can also be found for excitable systems in other fields of research.

We acknowledge S. Lepri and A. Politi for useful discussions and the European community for supporting T. K. via the Marie Curie Action Project No. 011434.

*Electronic address: thomas.kreuz@fi.isc.cnr.it

[1] L. Gammaitoni *et al.*, Rev. Mod. Phys. **70**, 223 (1998).
[2] Hu Gang *et al.*, Phys. Rev. Lett. **71**, 807 (1993).
[3] A. S. Pikovsky and J. Kurths, Phys. Rev. Lett. **78**, 775 (1997).
[4] B. Lindner *et al.*, Phys. Rep. **392**, 321 (2004).
[5] E. Manjarrez *et al.*, Neurosci. Lett. Suppl. **326**, 93 (2002).
[6] R. FitzHugh, Biophys. J. **1**, 445 (1961).
[7] J. M. Buldú *et al.*, Phys. Rev. E **64**, 051109 (2001).
[8] S. Brugioni *et al.*, Phys. Rev. E **71**, 062101 (2005).
[9] V. Beato *et al.*, Phys. Rev. E **71**, 035204(R) (2005).
[10] J. M. Casado, Phys. Lett. A **235**, 489 (1997).
[11] M. N. Shadlen and W. T. Newsome, J. Neurosci. **18**, 3870 (1998).
[12] E. Salinas and T. J. Sejnowski, J. Neurosci. **20**, 6193 (2000).
[13] M. Rudolph and A. Destexhe, Phys. Rev. Lett. **86**, 3662 (2001).
[14] J. Feng and P. Zhang, Phys. Rev. E **63**, 051902 (2001).
[15] R. Moreno *et al.*, Phys. Rev. Lett. **89**, 288101 (2002).
[16] W.-J. Rappel and S. H. Strogatz, Phys. Rev. E **50**, 3249 (1994).
[17] J. R. Pradines, G. V. Osipov, and J. J. Collins, Phys. Rev. E **60**, 6407 (1999).
[18] We use a fourth order Runge-Kutta integration scheme with time step $\delta t = 10^{-4}$. A spike is identified whenever $W(t)$ overcomes a fixed detection threshold $\Theta = 0.4$.
[19] First, the correlation ρ_x is chosen, and then σ^2 is fixed (independently of ρ_x) by selecting the appropriate number of synapses N.
[20] The observed CR effects cannot simply be due to the dependence of the output rate on the level of noise, since for any fixed degree of correlation the rate increases strictly monotonously with the noise strength.
[21] This quantity can be evaluated for the deterministic FHN model as the ratio $r(a) = 1 - T_{\mathrm{ref}}(a)/T_f(a)$, where $T_f(a) = 1/\nu_f(a)$ is the period of tonic firing for Eq. (1) with $I \equiv 0$ and $T_{\mathrm{ref}}(a)$ the refractory period estimated as the time needed to recover after a spike emission from $(V, W) = (1, 2/3)$ to the fixed point.
[22] E. Zohary, M. N. Shadlen, and W. T. Newsome, Nature (London) **370**, 140 (1994).
[23] E. Salinas and T. J. Sejnowski, Nat. Rev. Neurosci. **2**, 539 (2001).
[24] P. H. E. Tiesinga *et al.*, J. Physiol. (Paris) **98**, 296 (2004).